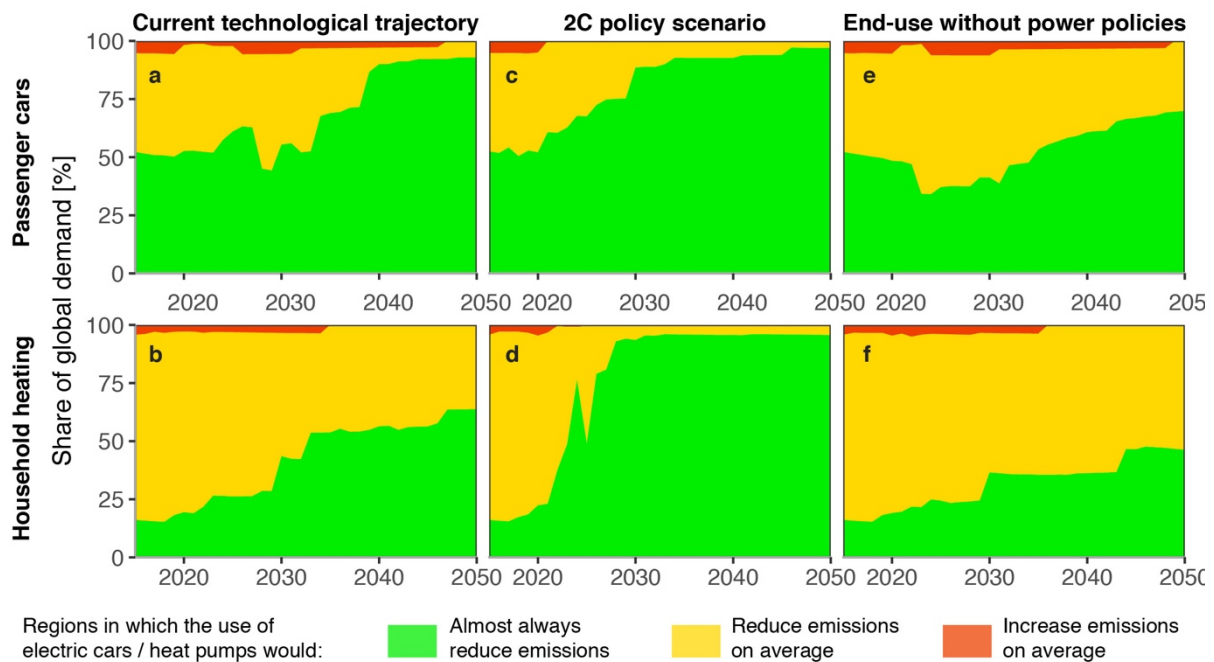


Supplementary information to:

Net emission reductions from electric cars and heat pumps in 59 world regions over time

Florian Knobloch^{1,2,*}, Steef Hanssen¹, Aileen Lam^{2,3}, Hector Pollitt^{2,4}, Pablo Salas², Unnada Chewpreecha⁴, Mark A. J. Huijbregts¹, Jean-Francois Mercure^{5,1,2,4}

1. Figures



SI-Fig. 1 Share of world in which electric cars and heat pumps are less GHG emission intensive. Fraction of global demand for passenger road transport (top) and household heating (bottom) attributable to world regions in which electric cars / heat pumps have lower projected life-cycle GHG emissions than new petrol cars / fossil boilers in almost all cases ('green') or on average ('yellow'), or are more GHG emission intensive on average ('red'). Projected shares under the 'current technological trajectory'; (a-b), the '2°C policy scenario' (c-d), and under a scenario in which the 2°C policies are applied to transport and heating, but power generation follows the 'current technological trajectory' ('end-use without power policies'; e-f).

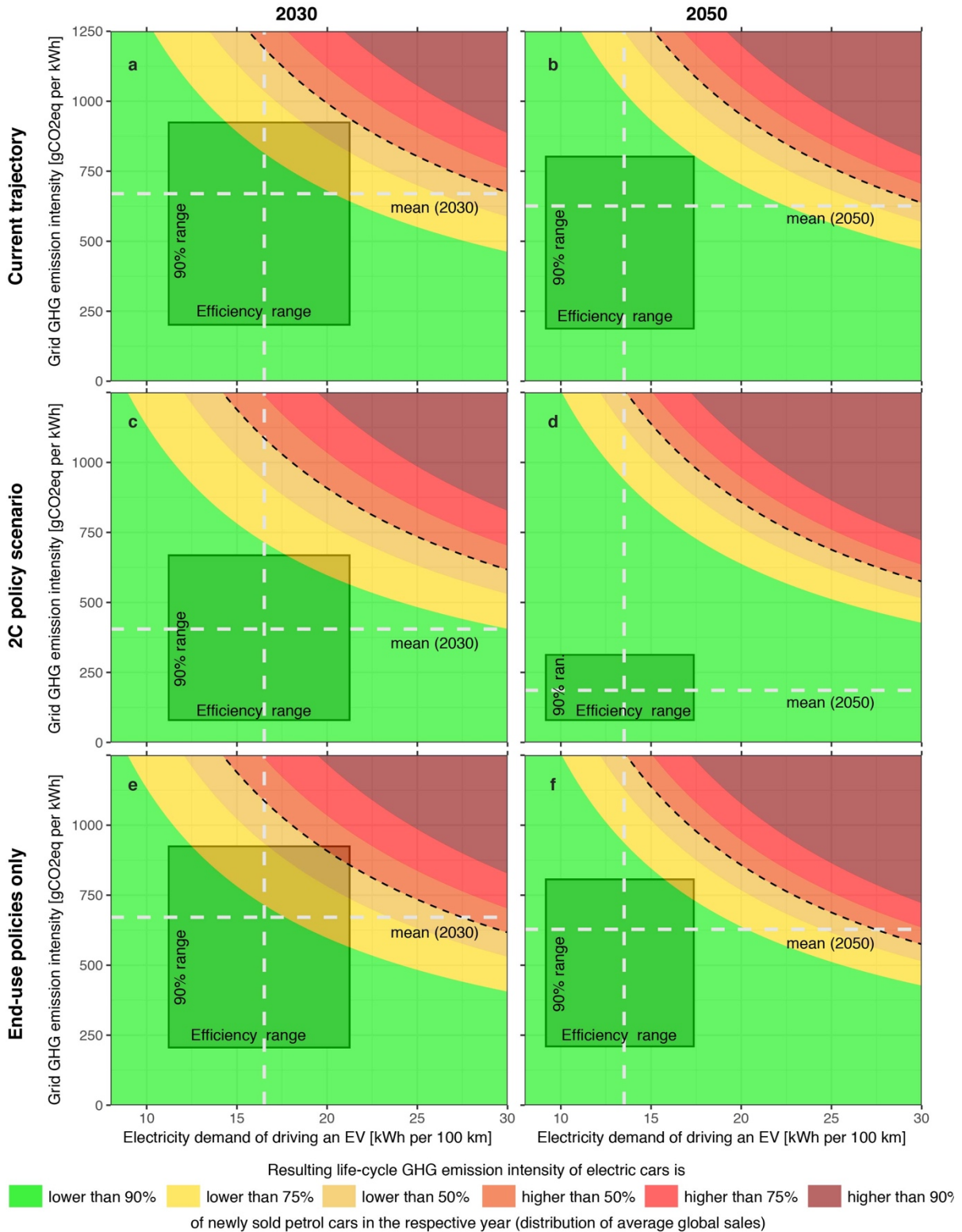
¹ Department of Environmental Science, Faculty of Science, Radboud University, Nijmegen, The Netherlands

² Cambridge Centre for Environment, Energy and Natural Resource Governance (C-EENRG), University of Cambridge, Cambridge, UK

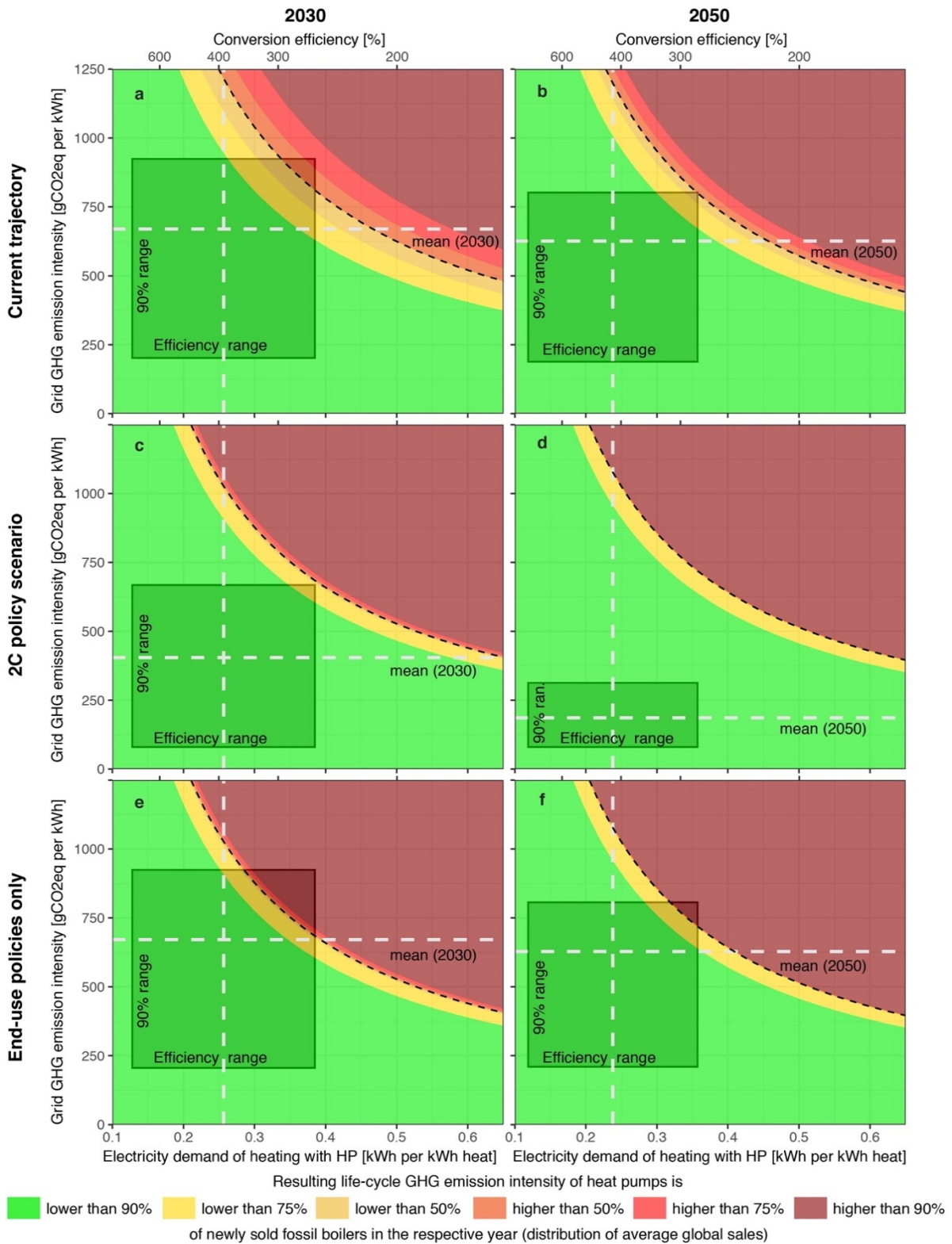
³ Department of Economics, Faculty of Social Sciences, University of Macao, Taipa, Macau

⁴ Cambridge Econometrics Ltd, Cambridge, UK

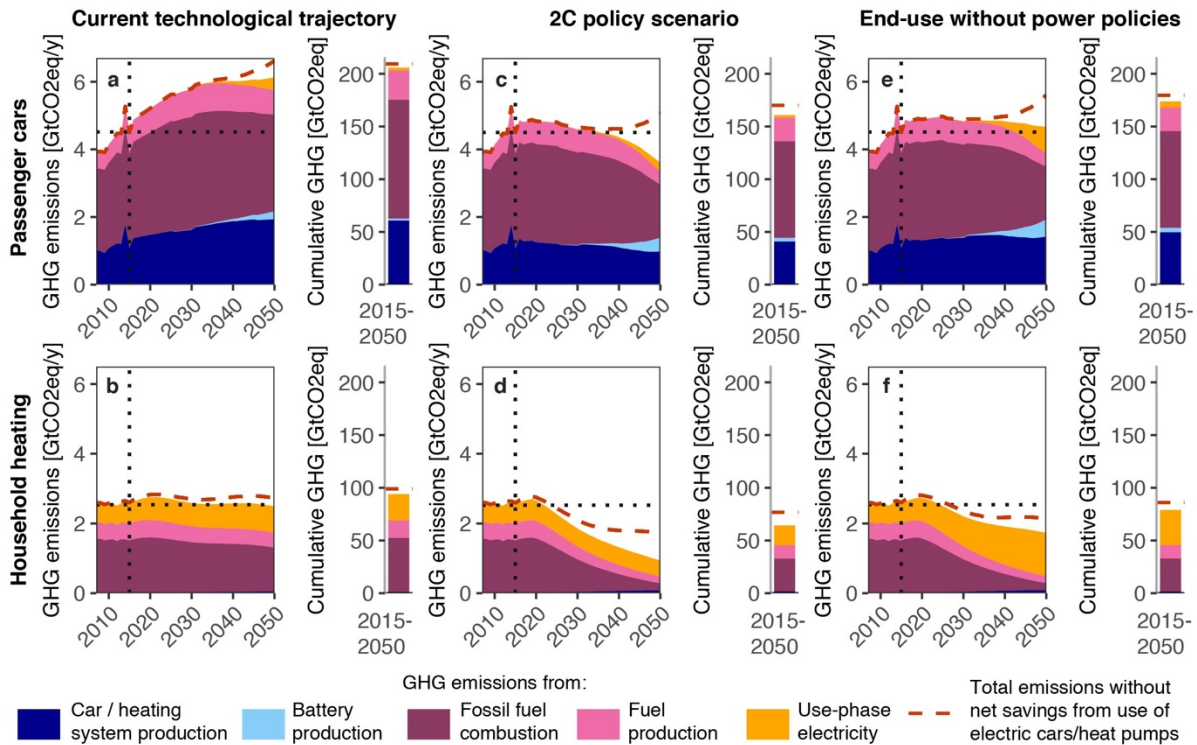
⁵ Department of Geography, College of Life and Environmental Sciences, University of Exeter, Exeter, UK



SI-Fig. 2 Boundary conditions for electric cars. Projected conditions (in 2030 and 2050) under which the life-cycle GHG emission intensities from driving electric cars (EV) is lower compared to new petrol cars being sold in the market, given different combinations of use-phase electricity demand and the electricity grid's GHG emission intensity in the respective year and scenario. Horizontal white lines indicate the average emission intensity of global electricity generation, vertical dashed lines the estimates of average EV use-phase efficiencies. Boxes indicate the 90% range of the electricity grid's GHG emission intensity and the 90% range of estimated EV use-phase efficiencies in the given year.



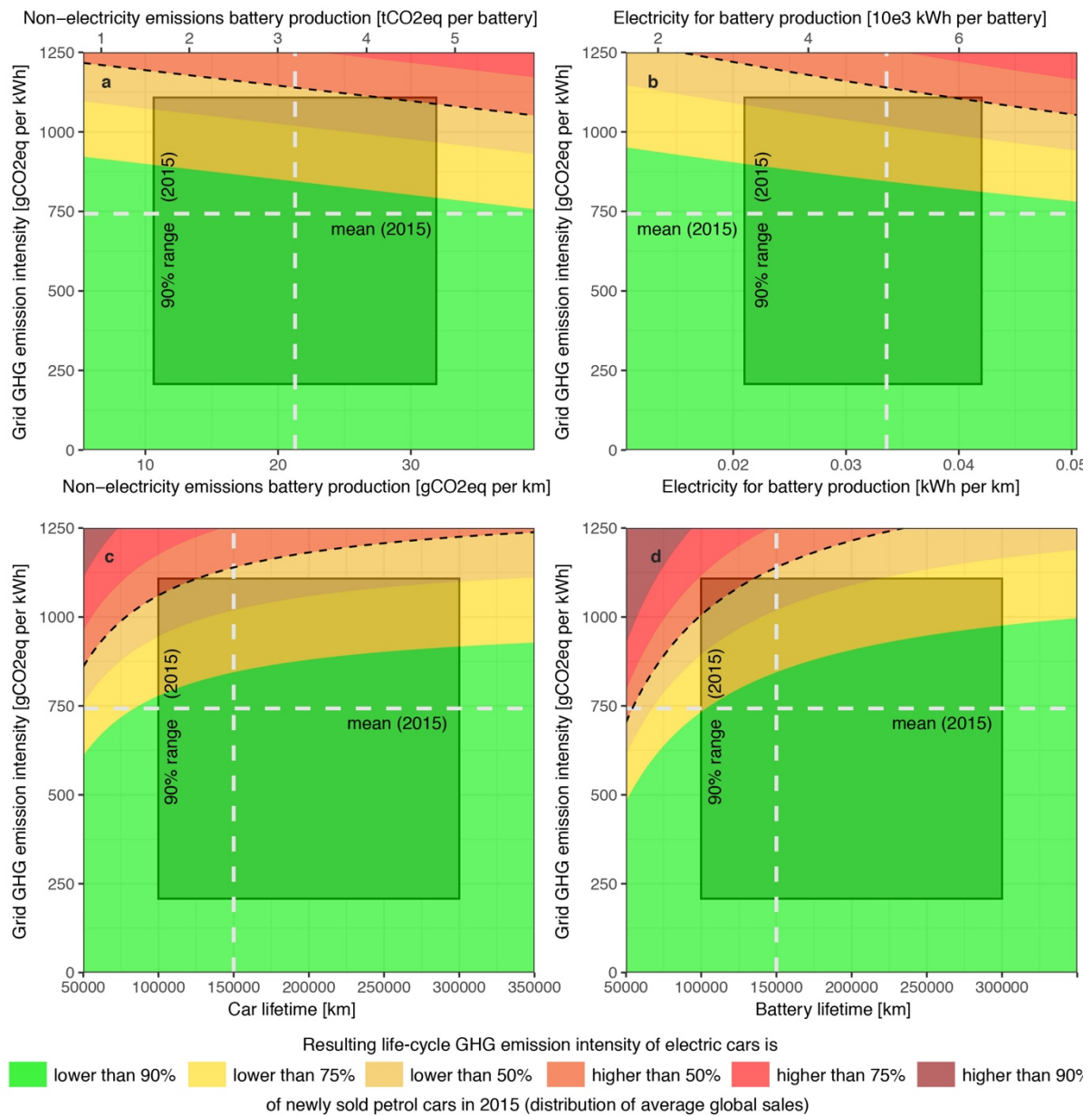
SI-Fig. 3 Boundary conditions for electric heat pumps. Projected conditions (in 2030 and 2050) under which the life-cycle GHG emission intensities from heating with electric heat pumps (HP) are lower compared to new fossil boilers being sold in the market, given different combinations of use-phase electricity demand and the electricity grid's GHG emission intensity in the respective year and scenario. Horizontal white lines indicate the average emission intensity of global electricity generation, vertical dashed lines indicate the estimates of average HP use-phase efficiencies. Boxes indicate the 90% range of the electricity grid's GHG emission intensity and the estimated range of HP use-phase efficiencies.



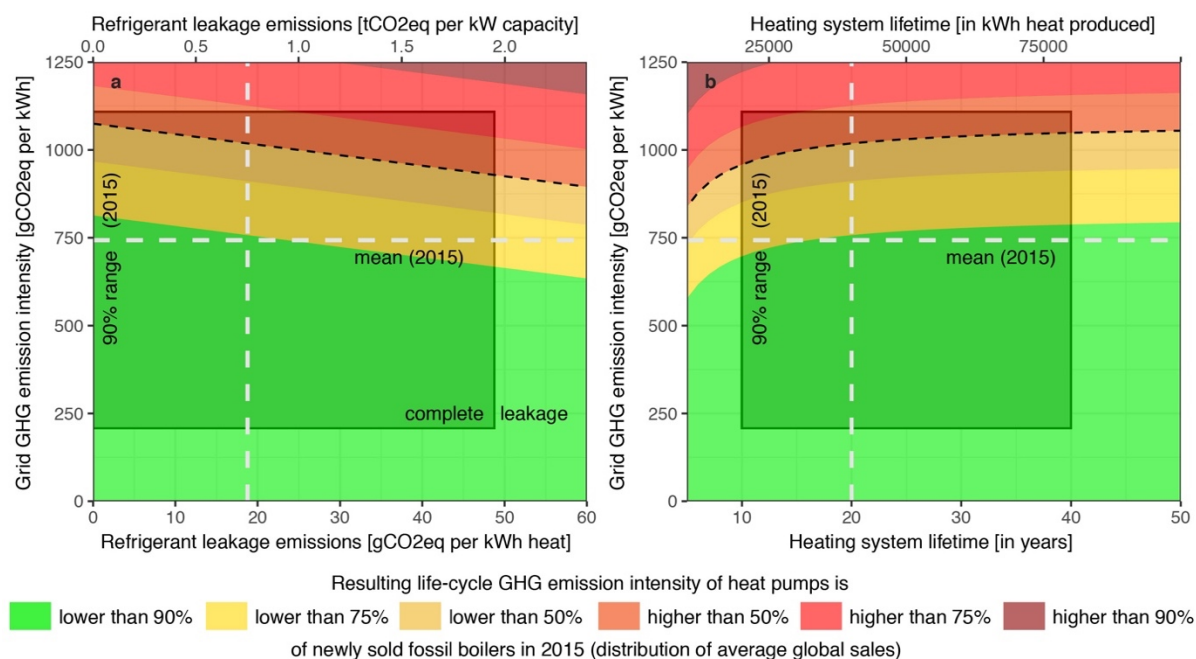
SI-Fig. 4 Projections of global GHG emissions from passenger cars and household heating. Direct GHG emissions from fossil fuel combustion (dark purple), indirect GHG emissions from fuel production (light purple) and use-phase electricity generation (orange), and GHG emissions from the production of cars and heating systems (dark blue, batteries for electric cars in light blue). Red dashed lines indicate levels of total GHG emissions without the use of any electric cars/heat pumps, if petrol cars and fossil boilers would be used instead. Projections under the ‘current technological trajectory’ (a-b), the ‘2°C policy scenario’ (c-d), and under a scenario in which the 2°C policies are applied to transport and heating, but power generation follows the ‘current technological trajectory’ (‘end-use without power policies’; e-f).

Total emissions were calculated as the sum of direct use-phase emissions (tailpipe emissions from driving petrol cars, on-site emissions from burning fossil fuels for heating), indirect use-phase emissions (from producing the required electricity or fuels), and emissions from the production and end-of-life of cars and heating systems (allocated to the respective years of production and scrapping). All emissions were estimated bottom-up, based on the projected emission intensities and demand for road transport (with passenger cars) and household heating (space and sanitary water). The resulting bottom-up estimates can be smaller than top-down emission estimates from IEA fuel use data, which also includes other end uses (such as freight transport or cooking). For the use of biomass/biofuels in heating and transport (according to the policy-defined blend), indirect emissions from their production and resulting land-use changes were added in the category ‘production of fuels’ (assuming an average emission intensity of 59 gCO₂eq/kWh of energy content for biomass used in heating, and of 99 gCO₂eq/kWh of energy content for biofuel used in transport⁵⁴).

2. Sensitivity analysis



SI-Fig. 5 Sensitivity analysis for boundary conditions of electric cars. Conditions under which the life-cycle GHG emission intensities from driving electric cars (EV) would currently be lower compared to new petrol cars being sold in the market, given different combinations of the electricity grid's GHG emission intensity and (a) non-electricity emissions from battery production, (b) electricity required for battery production, (c) car lifetime (of electric cars incl. battery and petrol cars), and (d) battery lifetime. Horizontal white lines indicate the average emission intensity of global electricity generation (in 2015), vertical dashed lines the default estimates (in 2015). Boxes indicate the range of car and battery variables (in 2015), which are based on Cox et al.¹, and the 90% range of the electricity grid's GHG emission intensity. All parameters which are not explicitly analyzed in the respective graph are set to their default values (for 2015).



SI-Fig. 6 Sensitivity analysis for boundary conditions of electric heat pumps. Conditions under which the life-cycle GHG emission intensities from heating with electric heat pumps (HP) would currently be lower compared to new fossil boilers being sold in the market, given different combinations of the electricity grid's GHG emission intensity and (a) GHG emissions from the leakage of refrigerant liquid (during production, use-phase and end-of-life), (b) lifetimes of heating systems. Horizontal white lines indicate the average emission intensity of global electricity generation (in 2015), vertical dashed lines the default estimates (in 2015). Boxes indicate the range in refrigerant leakage emissions and heating system lifetime (in 2015) and the 90% range of the electricity grid's GHG emission intensity. Potential emissions for the worst-case scenario of complete leakage are based on Mattinen et al.², ranges for heating system lifetime are based on Henkel³. All parameters which are not explicitly analyzed in the respective graph are set to their default values (for 2015).

3. Estimation of service demand for transport and heating

3.1 Demand for passenger car road transport

Future demand for passenger car road transport up to 2050 is endogenously determined by E3ME, by means of a regression estimate which is based on empirical relationships between observed demand, economic activity and fuel costs⁴⁻⁶. For each world region, the model regresses the vehicle travel demand (in passenger-km/year) with respect to fuel prices and income, both of which are also endogenously determined by E3ME. We use elasticities from the literature to constrain regression parameters and avoid spurious results.

Multiple regression analysis is used as an econometric technique used for investigating the relationship between transport demand, fuel price and household income. We estimate and project transport demand under different scenario assumptions, for given projections of the independent variables, which are estimated endogenously within the E3ME model.

Equation 1 shows the econometric specification for estimating future demand for passenger kilometres in region j :

$$PM_j = \alpha_{1,j} * RRPD_j + \alpha_{2,j} * PFRM_j + \varepsilon_j \quad (1)$$

PM is the demand for passenger car road transport in passenger kilometres in region j , $RRPD$ is the average real income of households in region j , and $PFRM$ is the end-user price of middle distillates for road transport in region j . $\alpha_{1,j}$ and $\alpha_{2,j}$ are the regression coefficients in region j , and ε_j is the regression error term. The regression coefficients of the model are estimated using the ordinary least square method, minimizing the sum of squared errors between the predicted travel demand (PM_j) and the observed historical travel demand in our dataset.

End-user fuel prices are inclusive of taxes, and are endogenously updated by E3ME within every year of the model simulation, reflecting changes in policy assumptions and endogenously evolving marginal costs of middle distillates (determined by a fossil-fuel supply model). Under different policy scenarios, the uptake of more efficient transport technologies as a result of more stringent policies can impact the demand for oil. Lower oil prices are consistent with a future of strong technological change (and hence lower oil demand), while high oil prices represent a future with lower diffusion of new efficient energy technologies (and hence higher oil demand).

Demand profiles show a substantial variation across regions. Generally, regions with fast growing economies (e.g. China, India, Brazil) also have a faster growing demand for transport (and thus also a higher response to price changes), compared to slow-growing developed economies (e.g. UK, USA). In our policy scenarios, endogenously decreasing oil prices on their own would be projected to result in slightly higher transport demand. However, the policy mix also assumes the introduction of new end-user fuel taxes, which results in a lower projected transport demand, compared to the 'current technological trajectory'.

3.2 Demand for residential space and water heating

Future changes in the demand for residential space and water heating in each region are based on estimates from the IMAGE-REMG model, following the methodology described in Isaac and van Vuuren⁷ and Daiglou et al.⁸. Demand for residential heating is defined in terms of useful energy (i.e., heat generated), and projected separately for space and water heating. Future demand for space heating in region j ($UE_{space,j}$) is projected based on equation 2:

$$UE_{space,j} = POP_j \times FS_j \times HDD_j \times HI_j \quad (2)$$

Here, POP is the population, FS is the available floor space per person (m^2/cap), HDD are heating degree days ($^{\circ}C$ days), HI is the useful energy heating intensity per floor area ($UE/m^2/HDD_j$) in region j . Floor space is an intermediate driver, estimated as a function of income and population density. Heating degree days are derived from monthly mean temperatures in the respective regions, considering future levels of global warming.

Future demand for water heating per person in each region is estimated as a function of income, and assumed to converge to a maximum saturation value, depending on heating degree days in the respective region⁸.

All future changes in population levels, climatic conditions and income are based on the SSP (Shared Socioeconomic Pathway) 2 scenario ('middle of the road')⁹, and all relevant data is publicly available via the IMAGE website (including future trends in FS , HDD and UE_{space})¹⁰. The space heating intensity of houses currently ranges from 50-150 $kJ_{UE}/m^2/HDD$, and foremost depends on heating practices and levels of building insulation. In our 'current technological trajectory' scenario, it is assumed that the heating intensity in all world regions decreases towards an average of 60 $kJ_{UE}/m^2/HDD$ by 2100 (or remains at current levels if these are lower). The assumption implies that the aggregate insulation efficiency of buildings increases, for example in reaction to more stringent building regulations, and the resulting heating intensity roughly corresponds to the 'sub-optimal' scenario in the Global Energy Assessment¹¹. In the '2C policy scenario' and the 'End-use without power policies scenario', we assume that the average heating intensity decreases towards 45 $kJ/m^2/HDD$ in all regions by 2050. This would require rapid improvements in the thermal insulation of new houses and the existing building stock: For example, the Passive House standard requires a maximum space heating energy demand of 15 kWh/m^2 , which roughly translates to a maximum useful heating intensity of 20 $kJ/m^2/HDD$. In terms of aggregate heating intensity, reducing global heating intensity from 50-200 to 45 $kJ/m^2/HDD$ over a 30-year period is therefore very ambitious, and would mean that a large fraction of houses is retrofitted to passive house properties.

Estimated effects of retrofitting on space heating demand are largest in Western Europe and North America, where heat demand remains high, but is largely saturated. In regions with fast-growing economies (such as China), large demand increases for space and water heating are projected with continuously rising income, partly offsetting the parallel demand decreases from improved building efficiencies. In warmer world regions (where space heating demand is very low), demand increases mainly reflect a growing demand for water heating in reaction to increasing income, and is therefore unaffected by our assumptions on housing insulation.

4. Estimation of life-cycle electricity requirements

Electricity requirements of electric car production (excl. the battery), petrol car production, heat pump production and fossil boiler production were all based on Ecolnvent (v3.5) as outlined in the Methods section of the main text. These electricity requirements include the electricity inputs of the foreground process (e.g., production of the car) and of all background processes (production of parts and materials, transport, mining, etc.). Electricity requirements were determined using the SimaPro software with data from the Ecolnvent (v3.5) database, by summing the electricity requirements of all processes in the *process contribution* step that include "electricity production" or "co-generation" in their name.

5. Allocation of GHG emissions to production and end-of-life stages

For the calculation of net savings and absolute GHG emission levels over time (as shown in Fig. 6 and SI-Fig. 4), non-electricity GHG emissions and electricity required for the production process were subdivided between the different life-cycle phases according to the following relative shares, derived from the Ecolnvent (v3.5) database:

	Non-electricity GHG emissions (incl. refrigerant leakage for HPs)			Electricity requirements (excl. use-phase electricity demand)		
	Production	Use-phase	End-of-life	Production	Use-phase	End-of-life
Petrol cars	97%	---	3%	100%	---	0%
EVs	96%	---	4%	100%	---	0%
EV batteries	91%	---	9%	80%	---	20%
Fossil boilers	98%	---	2%	100%	---	0%
HPs	10%	73%	17%	100%	---	0%

Note that for HPs, non-electricity GHG emissions include the leakage of refrigerant liquid during the use-phase and end-of-life stage, which account for the majority of overall HP non-electricity GHG emissions (see Methods).

References

1. Cox, B., Mutel, C. L., Bauer, C., Mendoza Beltran, A. & van Vuuren, D. P. Uncertain Environmental Footprint of Current and Future Battery Electric Vehicles. *Environ. Sci. Technol.* **52**, 4989–4995 (2018).
2. Mattinen, M. K., Nissinen, A., Hyysalo, S. & Juntunen, J. K. Energy Use and Greenhouse Gas Emissions of Air-Source Heat Pump and Innovative Ground-Source Air Heat Pump in a Cold Climate. *J. Ind. Ecol.* **19**, 61–70 (2014).
3. Henkel, J. Modelling the diffusion of innovative heating systems in Germany—Decision criteria, influence of policy instruments and vintage path dependencies. (2011).
4. Cambridge Econometrics. E3ME Manual, Version 6. (2014). Available at: <https://www.camecon.com/wp-content/uploads/2016/09/E3ME-Manual.pdf>.
5. Mercure, J.-F. *et al.* Environmental impact assessment for climate change policy with the simulation-based integrated assessment model E3ME-FTT-GENIE. *Energy Strateg. Rev.* **20**, 195–208 (2018).
6. Mercure, J.-F., Lam, A., Billington, S. & Pollitt, H. Integrated assessment modelling as a positive science: private passenger road transport policies to meet a climate target well below 2 °C. *Clim. Change* (2018). doi:10.1007/s10584-018-2262-7
7. Isaac, M. & van Vuuren, D. P. Modeling global residential sector energy demand for heating and air conditioning in the context of climate change. *Energy Policy* **37**, 507–521 (2009).
8. Daioglou, V., van Ruijven, B. J. & van Vuuren, D. P. Model projections for household energy use in developing countries. *Energy* **37**, 601–615 (2012).
9. Riahi, K. *et al.* The Shared Socioeconomic Pathways and their energy, land use, and greenhouse gas emissions implications: An overview. *Glob. Environ. Chang.* **42**, 153–168 (2017).
10. PBL. IMAGE User Support System. (2016). Available at: <http://themasites.pbl.nl/models/image/index.php/Download>.
11. Ürge-Vorsatz, D. *et al.* Energy End-Use: Buildings. in *Global Energy Assessment - Toward a Sustainable Future* 649–760 (2012).